Investigating the Accuracy of Mobile Urban Sensing

M. Fiore[†], A. Nordio[⋆], C.-F. Chiasserini[‡⋆]

[†] INSA Lyon and Inria, Lyon, France, [⋆] IEIIT-CNR, Torino, Italy, [‡] Politecnico di Torino, Torino, Italy

***Abstract*—Community urban sensing is one of the emerging applications enabled by the growing popularity of mobile user devices, like smartphones and in-vehicle monitoring systems. Such devices feature sensing and wireless communication capabilities, which enable them to sample large-scale phenomena, like air pollution and vehicular traffic congestion, and upload these data to the Internet. In this work, we focus on the above scenario and investigate the level of accuracy that can be achieved in estimating the phenomenon of interest through a mobile crowdsourcing application. Specifically, we take a signal processing-based approach and leverage results on signal reconstruction from sets of irregularly spaced samples. We apply such results to a realistic scenario where samples are collected by vehicular and pedestrian users, and study the accuracy level of the phenomenon estimation as the penetration rate of the sensing application varies.**

I. Introduction

Handhandled user devices, such as smartphones and tablets, as well as in-vehicle sensors are becoming extremely popular and represent a fertile ground for the development of crowdsensing (or, equivalently, community urban sensing) applications. Indeed, user devices are typically equipped with cameras, gyroscope, air-quality sensor, and accelerometer [1], [2]. The data obtained through such devices, as well as the ones gathered by in-vehicle sensors, can be combined with cellular BS positioning or GPS so as to obtain geo- and time-referenced samples of the urban environment. Cellular and WiFi interfaces can then be used, either interactively or autonomously, to transfer the user-generated data to the Internet, where they can be collected and processed. From such samples, it is therefore possible to estimate a large-scale phenomena of interest, such as air quality, noise level, as well as road traffic and vehicle speed [1], [2].

Clearly, urban sensing applications pose several challenges, including user privacy guarantees, data credibility, incentives to users for employing crowdsensing applications and efficient use of the wireless resources for uploading data to the Internet. The latter two aspects in particular are related to the amount of information that should be collected and processed in order to estimate the phenomenon of interest accurately enough.

In this work, we focus on such an aspect and aim at identifying the number of samples that should be collected through handhelded devices as well as in-vehicle sensors, and transferred wirelessly to a processing center so that the phenomenon is reconstructed with an acceptable error.

To do so, we take a signal processing approach and consider the problem of reconstructing the phenomenon (i.e., signal) from a set of samples that have been collected at irregular points in space, i.e., at the user/vehicle locations. Given the sample distribution, we apply a signal reconstruction method and evaluate the mean square error (MSE) between the original and the estimated phenomenon. We therefore investigate the dependency of the estimate accuracy on the number of samples, the phenomenon characteristics and the level of noise affecting the collected samples.

We evaluate our technique in the urban area of downtown Cologne, Germany, considering realistic city cartography and road traffic information [3]. Our results show the feasibility of our approach and yield interesting preliminary findings.

The rest of the paper is organized as follows. Section II introduces the methodology we follow to derive the accuracy achieved in reconstructing the phenomenon sensed through the crowsourcing application. Section III describes the real-world scenario under study and the spatial distribution associated to the samples collected through vehicular and pedestrian communication devices. Section IV shows the impact on the system performance of the penetration rate of the urban sensing application, among vehicular as well as pedestrian users. Finally, our concluding remarks can be found in Section V.

II. Signal reconstruction

The reconstruction of a signal from its discrete samples is a well known and widely investigated subject in the signal processing community. In particular, recent research activity has focused on the reconstruction of physical phenomena from irregularly spaced samples, such as those collected through mobile sensing devices. In the case where the samples are wirelessly sent to the Internet, a processing center can collect them and provide a reconstruction of the phenomenon of interest. The challenge here is to reconstruct the signal with a high level of accuracy, given the number of available samples, the noise level, and the signal spectral characteristics.

Let $s(x_1, x_2)$ be the physical phenomenon of interest, which should be monitored over a bi-dimensional region $\mathcal{R}$ of arbitrary size and shape. For simplicity, in this section we assume a square region of side 1, i.e., $\mathcal{R} = [0, 1)^2$, but a more general scenario can be considered without additional complexity. Let fix a time instant and assume that m devices, irregularly placed over the area $\mathcal{R}$, have provided the processing center with samples of the phenomenon. We denote the vector[1] including the m samples by $\mathbf{y} = [y_1, \ldots, y_m]^\mathsf{T}$. Considering that all devices are equipped with a positioning system (e.g., GPS),

This work was partially supported by the Self Organizing Networks research action of the INRIA and Alcatel-Lucent Bell Labs joint lab.

[1] Vectors and matrices are denoted by bold lowercase and uppercase letters, respectively. $\mathbf{I}$ represents the identity matrix; the superscripts $^\mathsf{T}$ and $^\mathsf{H}$ denote the matrix transpose and conjugate-transpose, respectively.

the spatial locations, at which the samples have been taken, i.e., $\mathbf{x}_q = [x_{1q}, x_{2q}] \in \mathcal{R}$, $q = 1, \ldots, m$, can be sent to the processing center along with the samples. Due to the mobility of pedestrian and vehicular users, we can consider the sampling points as instances of random variables with spatial distribution $f(z_1, z_2)$, $[z_1, z_2] \in \mathcal{R}$. Furthermore, the collected samples are typically affected by sensing noise and quantization inaccuracy; thus, they can be written as:

$$\mathbf{y} = \mathbf{s} + \mathbf{n}$$

where $\mathbf{s} = [s_1, \ldots, s_m]^{\mathsf{T}}$ is the vector of signal values at the sampling points ($s_q = s(\mathbf{x}_q)$) and $\mathbf{n} = [n_1, \ldots, n_m]^{\mathsf{T}}$ are the zero-mean random noise samples assumed to be uncorrelated with variance σ_n^2.

After receiving $\mathbf{y}$, along with the sampling locations $\mathbf{x} = [\mathbf{x}_1, \ldots, \mathbf{x}_m]^{\mathsf{T}}$, the processing center provides an estimate $\hat{s}(x_1, x_2)$ of $s(x_1, x_2)$. As a performance metric of the signal reconstruction, we take the mean square error (MSE) of the estimate, defined as:

$$\mathrm{MSE} = \mathbb{E}_{\mathbf{x}} \int_{\mathcal{R}} |\hat{s}(x_1, x_2) - s(x_1, x_2)|^2 \, \mathrm{d}x_1 \, \mathrm{d}x_2 \qquad (1)$$

where the average is taken with respect to the subscripted random vector.

In order to further elaborate the MSE in (1), we first note that any physical phenomenon can be approximated by a band-limited signal and written through its Fourier expansion as

$$s(x_1, x_2) = \frac{1}{n} \sum_{\ell_1=0}^{n-1} \sum_{\ell_2=0}^{n-1} a_{\ell_1 + n\ell_2} \mathrm{e}^{\mathrm{j}2\pi(\ell_1 x_1 + \ell_2 x_2)} \qquad (2)$$

where n is the approximate bandwidth (number of harmonics per dimension) of the signal, ℓ_1, ℓ_2 are integers taking values in $\{0, \ldots, n-1\}$, and $a_{\ell_1 + n\ell_2}$, $0 \leq \ell_1 + n\ell_2 \leq n^2 - 1$ denotes the signal spectrum coefficients. Using (2), we can write $\mathbf{y}$ as:

$$\mathbf{y} = \beta_{m,n}^{-1/2} \mathbf{V}^{\mathsf{H}} \mathbf{a} + \mathbf{n} \qquad (3)$$

where $\mathbf{a} = [a_0 \ldots a_{n^2-1}]^{\mathsf{T}}$ is the signal spectrum vector, $\mathbf{V}$ is an $n^2 \times m$ Vandermonde matrix with entries

$$(\mathbf{V})_{\ell_1 + n\ell_2, q} = m^{-1/2} \exp\left(-2\pi \mathrm{i}(\ell_1 x_{1q} + \ell_2 x_{2q})\right) \qquad (4)$$

and $\beta_{m,n} = n^2/m$. Since in general we do not have any information on the signal spectrum $\mathbf{a}$, we assume it is uncorrelated with zero mean and variance σ_a^2. Without loss of generality and for normalization reasons, we assume $\sigma_a^2 = 1$.

By using (2) in (1), we can rewrite the MSE as

$$\mathrm{MSE} = \mathbb{E}_{\mathbf{a},\mathbf{n},\mathbf{x}} \|\hat{\mathbf{a}} - \mathbf{a}\|^2 / n^2$$

where $\hat{\mathbf{a}}$ is an estimate of the signal spectrum $\mathbf{a}$. In the literature, many estimators of $\mathbf{a}$ have been proposed. Among these, linear estimators are commonly employed in signal detection and estimation since their analysis can be often carried out analytically. Here, we consider the linear minimum MSE (LMMSE) estimator, which provides the best performance among other linear estimators and is defined as:

$$\hat{\mathbf{a}} = \beta_{m,n}^{-1/2} \mathbf{V} \left(\beta_{m,n}^{-1} \mathbf{V}^{\mathsf{H}} \mathbf{V} + \sigma_n^2 \mathbf{I}\right)^{-1} \mathbf{y}.$$

By using this estimator in (1), the MSE becomes [5]

$$\mathrm{MSE} = \frac{1}{n^2} \mathbb{E}_{\mathbf{x}} \, \mathsf{Tr}\left(\gamma \beta_{m,n}^{-1} \mathbf{V}\mathbf{V}^{\mathsf{H}} + \mathbf{I}\right)^{-1} \qquad (5)$$

where $\gamma = 1/\sigma_n^2$ is the signal-to-noise ratio and $\mathsf{Tr}\{\cdot\}$ is the matrix trace operator. We recall that in (5) the matrix $\mathbf{V}$ is random since it depends on the random vector $\mathbf{x}$ through (4). The expression of the MSE is tightly connected to the η-transform of a random variable, defined as follows [4]:

Definition II.1. *The η-transform of a non-negative definite random matrix $\mathbf{A}\mathbf{A}^{\mathsf{H}}$, where $\mathbf{A}$ is $k \times h$ with aspect ratio $k/h = \alpha$ is given by:*

$$\eta_{\mathbf{A}}^{(h,k)}(\alpha, \gamma) = \mathbb{E}_{\mathbf{A}} \frac{\mathsf{Tr}\left(\gamma \mathbf{A}\mathbf{A}^{\mathsf{H}} + \mathbf{I}\right)^{-1}}{k} = \sum_{i=1}^{k} \frac{\mathbb{E}\left[(1 + \gamma\lambda_i)^{-1}\right]}{k}$$

where γ is a non-negative real number and λ_i is the i-th eigenvalue of $\mathbf{A}\mathbf{A}^{\mathsf{H}}$.

By using the definition of the η-transform and by recalling that $\mathbf{V}$ is an $n^2 \times m$ non-negative definite random matrix, with aspect ratio $\beta_{m,n} = n^2/m$, from (5) we can write

$$\mathrm{MSE} = \eta_{\mathbf{V}}^{(m,n^2)} \left(\beta_{m,n}, \frac{\gamma}{\beta_{m,n}}\right).$$

Furthermore, since the number of sampling devices is large, a more interesting performance metric is the asymptotic MSE defined as $\mathrm{MSE}_\infty = \lim_{n,m \to \infty, n^2/m = \beta} \mathrm{MSE}$, i.e., where n, m go to infinity with constant ratio $\beta = n^2/m$. The rationale behind this choice is that MSE_∞ has been shown to be an excellent approximation of the MSE already for small values of m and n [5], and it can be handled much more easily than the MSE for finite values of m and n. Indeed, it turns out that

$$\mathrm{MSE}_\infty = \lim_{\substack{n,m \to \infty \\ n^2/m = \beta}} \eta_{\mathbf{V}}^{(m,n^2)} \left(\beta_{m,n}, \frac{\gamma}{\beta_{m,n}}\right) = \eta_{\mathbf{V}} \left(\beta, \frac{\gamma}{\beta}\right)$$

where, according to the definition of the η transform,

$$\eta_{\mathbf{V}}(\beta, \gamma/\beta) = \mathbb{E}_\lambda \left[(1 + \gamma\lambda)^{-1}\right]$$

and λ is a random variable distributed as the asymptotic eigenvalues of $\mathbf{V}\mathbf{V}^{\mathsf{H}}$. Since $\mathbf{V}$ depends on the sampling positions, which are distributed according to $f(z_1, z_2)$, in the following we refer to $\eta_{\mathbf{V}}$ as η_f. We then use a result appeared in [6] that links η_f to η_u, i.e., the η-transform of $\mathbf{V}\mathbf{V}^{\mathsf{H}}$ computed in the case where the sample locations are random variables with uniform distribution. We obtain:

$$\eta_f \left(\beta, \frac{\gamma}{\beta}\right) = 1 - |\mathcal{A}| + |\mathcal{A}| \int_0^\infty g(y) \eta_u \left(\frac{\beta}{y}, \gamma y\right) \mathrm{d}y \qquad (6)$$

where $g(y)$ is the first derivative of the cumulative density function $G(y)$ defined as

$$G(y) = |\mathcal{A}|^{-1} \left|\{[z_1, z_2] \in \mathcal{R} \,|\, f(z_1, z_2) \leq y\}\right|,$$

$|\mathcal{S}|$ denotes the Lebesgue measure of the set $\mathcal{S}$, and $\mathcal{A} = \{[z_1, z_2] \in \mathcal{R} | f(z_1, z_2) > 0\}$. The advantage of using (6) to compute the accuracy in reconstructing the phenomenon (i.e.,

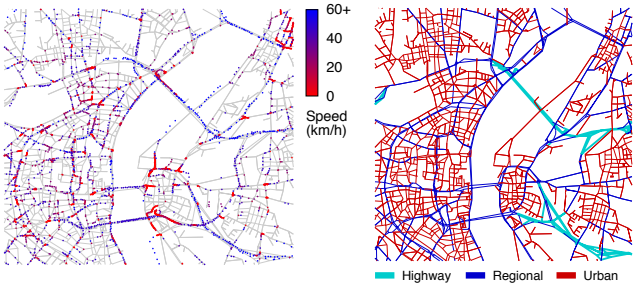

Fig. 1. Downtown Cologne road network: snapshot of the road traffic at 7 am (left) and layout of different road types (right, best viewed in colors).

the MSE_∞) is that the function η_u does not depend on the samples locations and can be easily computed numerically. In the next section, we specify how $g(y)$ can be obtained when the samples are collected through a urban sensing application.

III. Data set and empirical distribution

In order to evaluate our methodology to estimate the quality of the signal reconstruction in a practical scenario, we consider the case of downtown Cologne, Germany, assuming that vehicles traveling in the area are collecting the data required for the mobile urban sensing.

Our choice of the urban scenario is motivated by the availability of a large-scale synthetic dataset of the vehicular mobility in the region, that describes the road traffic of a 4500-km road network during 24 hours of a typical working day. The dataset includes per-second information on the position and speed of vehicles performing more than 700.000 trips [3].

The vehicular mobility is modeled through several state-of-art tools. The SUMO software, today's most advanced publicly-available microscopic vehicular mobility generator, is fed with the Cologne road layout collected from OpenStreetMap, i.e., the highest-quality free map database to date. The macroscopic flows of car traffic in the Cologne region, which are also provided as an input to SUMO, are determined in a two-phase process. Firstly, the Travel and Activity PAtterns Simulation (TAPAS) methodology [7] is applied to survey information collected in Cologne [8], so as to generate the travel demand (i.e., the origin and destination of each car trip). Secondly, the traffic assignment (i.e., the paths between each origin/destination pair) is derived through Gawron's relaxation algorithm [9], so as to reach a dynamic user equilibrium. Overall, such a generation process makes that of Cologne the largest and most complete vehicular mobility dataset freely available to date.

In our study, we focus on the downtown area of Cologne, a 25-km^2 area whose road network is portrayed in the left plot of Fig. 1. The picture shows a snapshot of the road traffic at 7 am, where each car is mapped onto a dot whose color corresponds to its current speed. We can observe the different traffic densities and speeds measured at different locations of the region.

We extracted from the Cologne mobility dataset the information about the position of vehicles, at different times of the day. We processed the position data so as to measure, for each of such daytimes, the intensity of the road traffic over the geographical area – which corresponds to the density of devices participating in the mobile sensing process.

Such a process was performed on different categories of roads separately. Indeed, downtown Cologne is traversed by a number of roads of heterogeneous nature that are characterized by dissimilar road traffic intensities. Therefore, the aggregate characterization of roads belonging to separate categories would lose information about the density of sensing devices on the different road types. Namely, we identified and treated separately three categories of roads. *Highway* roads include large high-speed motorways, that start or terminate close to the city center. *Regional* roads are major traffic arteries that cross and surround the downtown area. *Urban* roads represent the finer portion of the road network mesh, interconnecting regional roads and allowing to reach precise locations in downtown Cologne. A visual representation of the road classification is provided in the right plot of Fig. 1.

For each road category, we thus measured the geographic road traffic intensity (expressed in vehicles/km^2) as the ratio between the traffic volume at a specific road location (in vehicles) and the road surface at that location (in km^2). Clearly, the geographic road traffic intensity varies over daytime, as the traffic conditions change at different hours. Also, the intensity is affected by the vehicle penetration rate ρ_v, i.e., the fraction of cars equipped with sensing capabilities and participating in the crowdsensing process. Examples of the geographic road traffic intensity, observed over highway, regional and urban roads at 8 am and in presence of a penetration rate $\rho_v = 1$, are depicted in Fig. 2.

As previously mentioned, the geographic road traffic intensity corresponds to the spatial distribution of sensing devices, i.e., $f(z_1, z_2)$ in Sec. II. We thus leveraged it to derive the experimental $g(y)$, as defined at the end of Sec. II. Finally, the analytical expressions of the $g(y)$ required by (6) were obtained by fitting mixed normal/exponential distributions to the experimental data. The process was repeated for different combinations of road type, daytime and vehicle penetration rate. Examples of experimental $g(y)$ and of the associated fittings are provided in Fig. 3.

Finally, we consider that pedestrian mobile users can also participate in the urban sensing process through, e.g., their smartphones. We assume the pedestrian users to be uniformly distributed over the areas not covered by roads, with constant density ϕ_p users/km^2, and we denote by ρ_p the penetration rate of the sensing application among such users.

The $g(y)$ associated to vehicles on different roads and to pedestrians were then combined, by scaling each of these quantities by the fraction of the region occupied by the corresponding type of users.

IV. Results

Fig. 4(a) shows the MSE achieved when considering $n = 20$ harmonics per dimension in the representation of the measured signal, the experimental vehicular densities at 8 am, a density

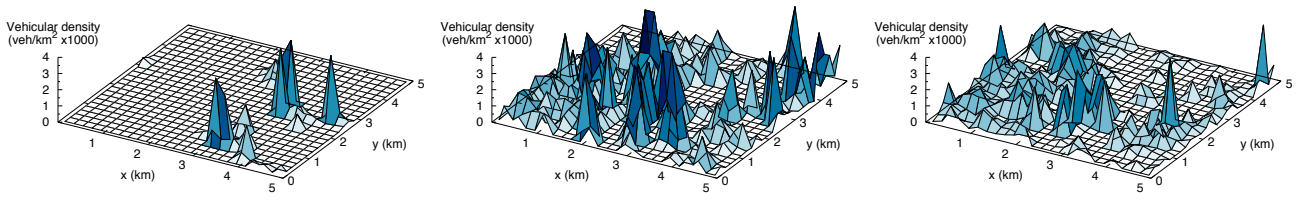

(a) Highway (b) Regional (c) Urban

Fig. 2. Geographic road traffic intensity in downtown Cologne, at 8 am and with a full penetration rate ($\rho_v = 1$), for the different road categories.

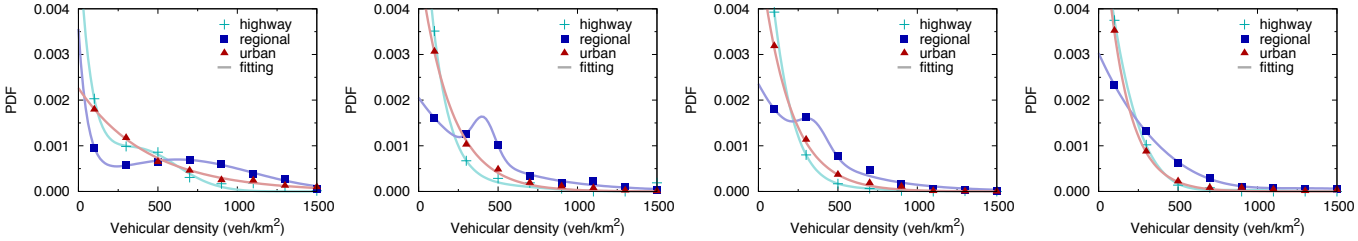

(a) 8 am, $\rho_v = 1.0$ (b) 8 am, $\rho_v = 0.5$ (c) 1 pm, $\rho_v = 1.0$ (d) 5 pm, $\rho_v = 0.5$

Fig. 3. Experimental and fitted mixed normal/exponential $g(y)$ for each road category for a selection of daytimes and penetration rates.

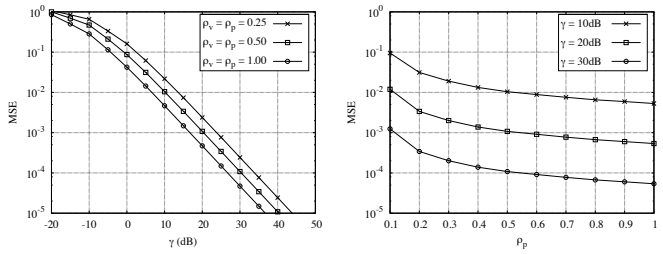

(a) (b)

Fig. 4. MSE achieved with $n = 20$, $\phi_p = 500$ users/km^2 and for (a) different values of $\rho_v = \rho_p$, and (b) $\rho_v = 0.5$ and varying ρ_p.

of pedestrian users $\phi_p = 500$ users/km^2, and identical penetration rates of the crowdsourcing application for both vehicular and pedestrian users, i.e., $\rho_v = \rho_p$. We observe that, as the penetration rate increases (i.e., the number of signal samples increases), the MSE decreases quite significantly. However, the MSE decrease is much more evident when the signal-to-noise ratio γ, i.e., the accuracy of the measurements collected by each mobile user, grows.

For the same system parameters and for $\rho_v = 0.5$, Fig. 4(b) shows the MSE as the penetration rate for pedestrian users, ρ_p, varies. As expected, the MSE decreases as ρ_p (i.e., the total number of samples) increases. More interestingly, most of the gain in terms of MSE is obtained by increasing ρ_p up to 0.5, while a larger penetration rate for pedestrian users does not provide any further significant reduction in the MSE.

V. Conclusion and Future Work

We considered a signal processing approach to solve the problem of assessing the accuracy of crowdsourced urban sensing. Results derived in a realistic scenario where both vehicular and pedestrian mobile users participate in the community sensing process show the feasibility of our approach. Preliminary findings are that (i) the accuracy of the measurements collected by the users is more critical than the sheer number of users, and (ii) a small number of pedestrian users is sufficient to significantly improve the quality of the urban sensing provided by vehicles only. Future work will consider the evaluation of our approach in more heterogeneous urban regions, and will aim at deriving a more comprehensive set of results and insights in the crowdsensing process.

References

[1] R.K. Ganti, Y. Fan Ye, L. Hui, "Mobile crowdsensing: current state and future challenges," *IEEE Comm. Mag.,* Vol. 49, No. 11, pp. 32-39, 2011.

[2] N.D. Lane, E. Miluzzo, H. Lu, D. Peebles, T. Choudhury, A.T. Campbell, "A survey of mobile phone sensing," *IEEE Comm. Mag.,* Vol. 48, No. 9, pp. 140-150, 2010.

[3] S. Uppoor, M. Fiore, "Large-scale urban vehicular mobility for networking research," *IEEE VNC,* 2011.

[4] A. Tulino and S. Verdú, *Random matrix theory and wireless communication,* Now Publishers, 2004.

[5] A. Nordio, C.-F. Chiasserini, E. Viterbo, "Performance of linear field reconstruction techniques with noise and uncertain sensor locations," *IEEE Trans. on Signal Proc.,* Vol. 56, No. 8, pp. 3535–3547, 2008.

[6] A. Nordio, C.-F. Chiasserini, "Field Reconstruction in Sensor Networks with Coverage Holes and Packet Losses," *IEEE Trans. on Signal Proc.,* Vol. 59, No. 8, pp. 3943-3953, 2011.

[7] G. Hertkorn, P. Wagner, "The application of microscopic activity based travel demand modelling in large scale simulations," *World Conference on Transport Research,* 2004.

[8] G. Rindsfüser, J. Ansorge, H. Mühlhans, "Aktivitätenvorhaben," in K.J. Beckmann (Ed.), *SimVV Mobilität verstehen und lenken – zu einer integrierten quantitativen Gesamtsicht und Mikrosimulation von Verkehr,* Final report, 2002.

[9] C. Gawron, "An Iterative Algorithm to Determine the Dynamic User Equilibrium in a Traffic Simulation Model," *International Journal of Modern Physics C,* Vol. 9, No. 3, pp. 393–407, 1998.